Expansion Dynamics in the One-Dimensional Fermi-Hubbard Model

J. Kajala, F. Massel, and P. Törmä

Phys. Rev. Lett. **106**, 206401 — Published 16 May 2011

DOI: 10.1103/PhysRevLett.106.206401

Expansion dynamics in the one-dimensional Fermi-Hubbard model

J. Kajala,[1] F. Massel,[2] and P. Törmä[1,3,*]

[1]*Department of Applied Physics, Aalto University School of Science, P.O.Box 15100, FI-00076 Aalto, FINLAND*
[2]*Low Temperature Laboratory, Aalto University, P.O. Box 15100, FI-00076 Aalto, FINLAND*
[3]*Kavli Institute for Theoretical Physics, University of California, Santa Barbara, California 93106-4030, USA*

(Dated: April 21, 2010)

Expansion dynamics of interacting fermions in a lattice are simulated within the one-dimensional (1D) Hubbard model, using the essentially exact time-evolving block decimation (TEBD) method. In particular, the expansion of an initial band-insulator state is considered. We analyze the simulation results based on the dynamics of a two-site two-particle system, the so-called Hubbard dimer. Our findings describe essential features of a recent experiment on the expansion of a Fermi gas in a two-dimensional lattice. We show that the Hubbard-dimer dynamics, combined with a two-fluid model for the paired and non-paired components of the gas, gives an efficient description of the full dynamics. This should be useful for describing dynamical phenomena of strongly interacting Fermions in a lattice in general.

PACS numbers: 71.10.Fd , 03.75.Ss, 73.20.Mf

Important physical phenomena such as magnetism and high-temperature superconductivity are often approached by theories based on the Hubbard model [1, 2] which describes interacting particles in a lattice. Within ultracold gas systems [3, 4], the Hubbard model can be efficiently realized and studied in experiments with bosonic [5] and recently with fermionic atoms [6, 7]. Intriguingly, the dimension can be easily controlled. Low-dimensional systems such as nanowires, iron pnictides and graphene are currently highlighted topics of research. Models for the quantum many-body physics of 2D and 1D systems can explored with ultracold gases, c.f. recent experiments on fermions in one dimension [8] and expanding fermions in a 2D lattice [9]. For one-dimensional systems, an advantage is that the experiments can be compared to exact theoretical descriptions. However, although the ground state and static properties of one-dimensional systems are known to an impressive degree [1, 11], *dynamics* is largely unexplored. Work on theory and simulation of dynamical properties of interacting fermions in 1D has recently been emerging [12].

In this Letter, we study with exact numerical methods the expansion of fermions within the one-dimensional Hubbard model. We show that the resulting complex dynamics can be efficiently described by a two-fluid model in which we deduce the dynamics of the fluids from the dynamics of a Hubbard dimer. Our results explain several main features of the experiment [9] performed in 2D, and give exact predictions for future experiments in 1D. The simple Hubbard-dimer two-fluid model that we have developed provides a basis for the description of various types of expansion, collision and oscillation dynamics for fermions in lattices.

We use the time-evolving block decimation (TEBD) algorithm [13] to describe the time evolution generated by the Hubbard Hamiltonian $H_H = U\sum_i \hat{n}_{i,\uparrow}\hat{n}_{i,\downarrow} - J\sum_{i\,\sigma=\uparrow,\downarrow} c^\dagger_{i\,\sigma}c_{i+1\,\sigma} + h.c.$, given an initial state $|\phi(0)\rangle$,

FIG. 1: (color online) Schematic representation of the initial state: the middle part of the lattice is fully occupied (O_i) and the rest is empty (E_i). Sites E_L, O_L and O_R, E_R represent the left and right edge of the cloud, respectively.

where $\hat{n}_{i,\sigma} = c^\dagger_{i\,\sigma}c_{i\,\sigma}$ with $c^\dagger_{i\,\sigma}$ and $c_{i\,\sigma}$ representing the creation and annihilation of a fermion with spin σ at the site $i = 1 \ldots L$. Moreover, the initial state is given by $|\phi(0)\rangle = |\emptyset\rangle_1 \ldots |\emptyset\rangle_{E_L} |\uparrow\downarrow\rangle_{O_L} \cdots |\uparrow\downarrow\rangle_{O_R} |\emptyset\rangle_{E_R} \ldots |\emptyset\rangle_L$ (see Fig. 1). The initial state consists thus of a band insulator occupying the central $O_L - O_R$ sites of an otherwise empty lattice. In the simulation we have considered $L = 150$, $E_L = 66$, $O_L = 67$, $O_R = 86$, $E_R = 87$, the Schmidt number $\xi = 150$, and $J = 1$. Our code allows us to access the expectation value of the (spin-resolved) local particle number $n_{i\uparrow}(t)$ and $n_{i\downarrow}(t)$ along with the local double occupancy $n_{i\uparrow\downarrow}(t) = \langle\phi(t)|\hat{n}_{i\uparrow}\hat{n}_{i\downarrow}|\phi(t)\rangle$. Note that $n_{i\downarrow}(t) = n_{i\uparrow}(t)$ since the problem is spin symmetric. In our analysis we will show that the evolution of the initial state can be described in terms of a two-fluid model where the two fluids are represented by single particles and *doublons* as suggested by the Bethe-ansatz solution of the Hubbard model [1] and has been shown in the context of imbalanced Fermi gases [14–18]. The doublons are excitations of the form $c^\dagger_{i\uparrow}c^\dagger_{i\downarrow}|\emptyset\rangle$ and the single (unpaired) particles are defined as $c^\dagger_{i\,\sigma}|\emptyset\rangle$ ($\sigma =\uparrow, \downarrow$). The local number of doublons is given by $n_{i\uparrow\downarrow}(t)$, while the number of unpaired (up) particles is given by $n^{un}_{i\uparrow}(t) = n_{i\uparrow}(t) - n_{i\uparrow\downarrow}(t)$.

In Figs. 2 and 3, $\sqrt{n_{i\uparrow}(t)}$ and $\sqrt{n_{i\uparrow\downarrow}(t)}$ are depicted for $U = 0.0$ and $U = \pm 10.0$. We are plotting the square roots of the densities since this highlights low density features (see the supplementary material for the full den-

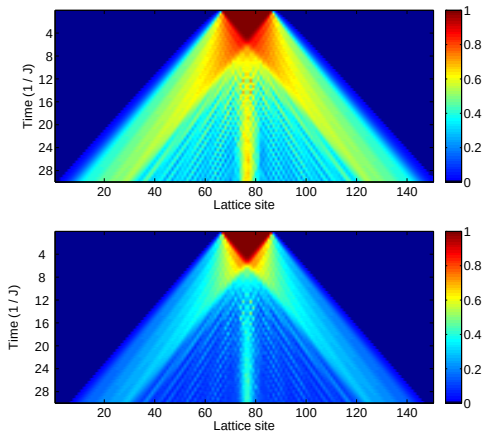

FIG. 2: (color online) Time evolution of $\sqrt{n_{i\uparrow}(t)}$ (above) and $\sqrt{n_{i\uparrow\downarrow}(t)}$ (below) for $|U| = 0.0$. The free-particle nature of the expansion is clear from the absence of separate doublon expansion wavefronts.

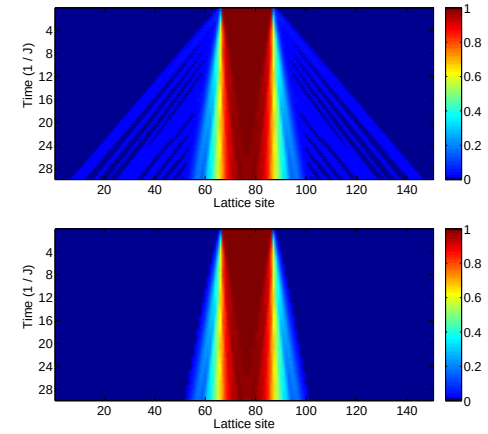

FIG. 3: (color online) Same as Fig. 2 for $|U| = 10.0$. For this interaction it is possible to distinguish the two wavefronts.

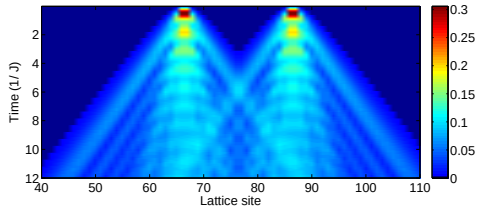

FIG. 4: (color online) Unpaired particle expansion $n^{un}_{i\uparrow}(t)$ for $|U| = 5.0$, exhibiting the oscillations described in the text.

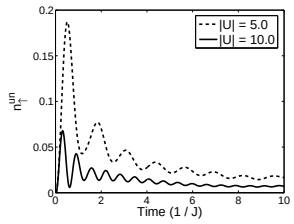

FIG. 5: Unpaired population dynamics $n^{un}_{E_L+O_L,\uparrow}(t)$ for $|U| = 5.0$ and $|U| = 10.0$.

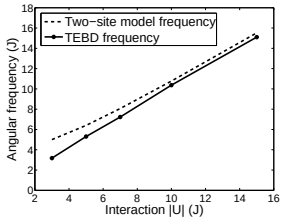

FIG. 6: The frequency given by the FT of $n^{un}_{E_L+O_L,\uparrow}(t)$ (from TEBD numerics) compared to the frequency $\sqrt{U^2+16J^2}$ obtained by solving the two-site model.

sity plots). As in general for the spin-balanced Hubbard model [1], the density distributions evolve in time exactly in the same way for U and $-U$. This $U \leftrightarrow -U$ symmetry holds also for all observables for all interactions and it was indeed observed also in the experiment [9].

In the non-interacting case in Fig. 2, both particles and doublons are expanding at the speed of $2J$, corresponding to the highest group velocity allowed by the dispersion relation (see supplementary material). For strong interactions (Fig. 3), we see two separate wavefronts. Such separation into two types of wavefronts is clearly observable for interactions $|U| > 3.0$. The outermost wavefront consists of fully unpaired particles expanding at the of speed $2J$, like in the $U = 0$ case. In contrast *doublons* expand at the speed of $4J^2/U$ (see supplementary material for the explanation of these results).

Intermediate interactions $0.5 \leq |U| \leq 3.0$ show a more complicated behaviour. The separate expansion fronts are no longer well distinguishable, suggesting a stronger interplay between single particles and doublons. Moving to even lower interactions, the unpaired particles and the doublons behave similarly to the case of $U = 0$. Let us now examine the time dependence of the number of unpaired (up) particles $n^{un}_{i\uparrow}(t)$ for $|U| = 5.0$ (Fig. 4). Initially the dynamics in the band insulator cloud is Pauli blocked, since neighbouring lattice sites in the center have unit density for both spin up and down. Therefore the unpaired expansion fronts are created at the edges of the cloud. Intriguingly, $n^{un}_{i\uparrow}(t)$ shows damped oscillations at the edges associated with the emission of unpaired particles into the empty lattice. Considering the time evolution of $n^{un}_{E_L,\uparrow} + n^{un}_{O_L,\uparrow}$ (the two edge sites) over the whole interaction range $|U| = 0.0 - 15.0$ (see Fig. 5 for $|U| = 5.0$, 10) we find that there are fewer periods of oscillations for lower interactions (for $|U| = 1.0$ only one broad oscillation peak is visible) and the oscillation frequency increases with interaction strength, see supplementary material for a general survey of the data.

The evolution of doublons into unpaired particles plays a key role in the expansion physics. For this reason, we focus now on the explanation of the oscillations in the case of high interactions, see Figs. 4 and 5. Our hypothesis is that one can consider the edges of the cloud (sites E_L, O_L and O_R, E_R) at short timescales as two-site systems (Hubbard dimers [1, 11]). Focusing on the E_L/O_L dimer, the system can be described as an initially empty state $|\emptyset\rangle$ in the left lattice site E_L and a doublon $|\uparrow\downarrow\rangle$ in the right lattice site O_L. The dynamics of the dimer with

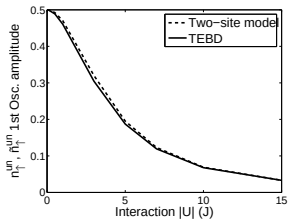

FIG. 7: The height of the first peak of $n^{un}_{E_L+O_L,\uparrow}(t)$ (from TEBD numerics) compared to the amplitude obtained by solving the two-site model.

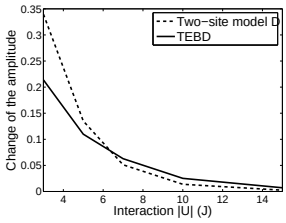

FIG. 8: Change of the amplitude of $\tilde{n}^{un}_{E_L,\uparrow}(t)$ oscillations after $t = \frac{3\pi}{\sqrt{U^2+16J^2}}$, compared to the change of amplitude between the first and second peaks of $n^{un}_{O_L+E_L,\uparrow}(t)$ observed in TEBD numerics.

this initial state can be solved analytically by diagonalizing its Hamiltonian (see supplementary material). As a result, in the two-site problem, the population of unpaired up particles on the two sites E_L and O_L is given by (the tilde refers to the Hubbard dimer model):

$$\tilde{n}^{un}_{E_L+O_L,\uparrow}(t) = \frac{1-\cos(\sqrt{U^2+16J^2}t)}{2+\frac{U^2}{8J^2}}. \qquad (1)$$

We extract the oscillation frequencies from the numerical Fourier transform (FT) of $n^{un}_{E_L+O_L,\uparrow}$ and compare its peaks to the oscillation frequency $\sqrt{U^2+16J^2}$ in (1) (see Fig. 6). Moreover, we compare the height of the first peak of the unpaired density oscillations (seen in Figs. 4 and 5) to the amplitude $8/\left(16+\frac{U^2}{J^2}\right)$, in Fig. 7.

The agreement is good considering that, for longer times, the FT of $n^{un}_{E_L+O_L,\uparrow}(t)$ has additional contributions stemming from the hopping between the dimer and the rest of the chain. However, as the frequency is approximately U in the high interaction limit, one might claim that the frequency correspondence could be obtained from simple energy arguments. Therefore, to further confirm the validity of the Hubbard Dimer model, we now move on to examine whether the two-site model coupled to the next adjacent sites explains the decay observed in $n^{un}_{E_L+O_L,\uparrow}(t)$ (see Fig. 5). Let us define the damping D to mean the decrease of the amplitude of the unpaired density oscillations, compared to $t = 0$. We propose that the damping should be equal to the probability of having an unpaired particle in the Hubbard dimer times the probability for this single particle tunnelling out of this system. The probability for the single particle tunnelling (obtained by solving the two-site system with the initial state $|\emptyset,\uparrow\rangle$) is given by $\sin^2(J\,t)$. Combining this result with Eq.(1), we obtain the damping at a given time τ:

$$D(\tau) = 2\int_0^\tau \frac{1-\cos(\sqrt{U^2+16J^2}t)}{2+\frac{U^2}{8J^2}}\sin^2(J\,t)dt, \qquad (2)$$

where the factor of two comes from the particle-hole symmetry: particles leaking out from the dimer to the left (to E_L-1) are mirrored by holes leaking to the right (to O_L+1) thus generating particle-like expansion fronts emitted out of the initial cloud and hole-like expansion fronts emitted into the cloud. When the particle-like and hole-like expansion fronts meet interference in the unpaired particle density is visible, see Fig. 4.

By comparing the decay predicted in Eq. (2) to the numerics, we observe that, for the duration of the first half-period, the decay is negligible. This is in accordance with the height of the first peak being equal to the two-site oscillation amplitude, as shown in Fig. 7. After three half-periods we compare the damping as predicted by Eq. (2) to the change of amplitude between the first peak and the second peak seen in numerics, see Fig. 8. The two-site model is again in good agreement with TEBD for $|U| > 3.0$. The time beyond which Eq. (2) fails to describe the expansion physics is when the population of unpaired particles in the sites O_{L+1}, E_{L-1} becomes significant. This occurs when the $sin^2(Jt) = \frac{1-2cos(2Jt)}{2}$ term is no longer close to zero, limiting our short time analysis to times $t << \frac{\pi}{2}\frac{1}{J}$. When U is sufficiently large, the Hubbard dimer oscillations occur in much shorter timescale than the single particle tunneling does. In other words, a large number of oscillations occur in the window $0 < t < \frac{\pi}{2}\frac{1}{J}$ In the case of lower interactions, Hubbard Dimer oscillations at frequency $\sqrt{U^2+16J^2}$ become comparable to the frequency $2J$ and therefore we see that already the first oscillation peaks are heavily damped.

In general, the two-site dynamics is well able to describe the creation of the particle, hole, and doublon wavefronts seen in the density profiles. These wavefronts are created during the two-site oscillations. Our numerical results and analytical investigations confirm the two-fluid picture of the system. Initially, the interaction takes place at the edges of the cloud, where unpaired particles are created according to the dimer dynamics described above. The subsequent expansion is explained by dynamics of non-interacting particles (at the speed of $2J$) or doublons (at the speed of $4J^2/U$). Our model gives an excellent quantitative description in the highly-interacting limit due to the clear separation of the expansion and dimer oscillation eigenfrequencies. For interactions $0.5 \leq |U| \leq 3.0$ the interplay between the expansion and the Hubbard dimer dynamics does not allow a quantitative description of the numerical results, however it provides a qualitative framework for further analysis. For $|U| \leq 0.5$, the free-particle expansion seems to give a fairly good description.

Finally, we compare our results to the 2D experiment of [9] done at finite temperature. We suggest that our two-site considerations also apply to the dynamics of the experiment. In 2D there is coupling to four adjacent sites, but just like in 1D, initially the sites are either Pauli

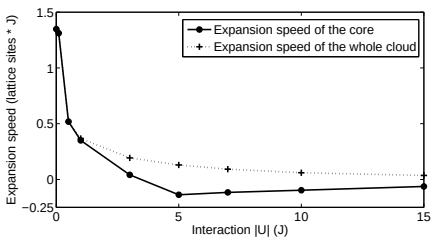

FIG. 9: The core expansion speed $\dot{R}(t)$, as a function of the interaction strength. For reference, we plot also the expansion speed of the whole cloud.

blocked or empty. The simplified dynamics should originate from the two-site analysis, and subsequent short-time dynamics in the high interaction limit correspond to the two-fluid expansion, with the two fluids interacting only at the edges.

In order to compare our results to Fig. 5 of [9] we define the core density as $n^C_{i\uparrow}(t) = n_{i\uparrow}(t) - n^b_{i\uparrow}(t)$ for $|U| > 0.5$ and $n^C_{i\uparrow}(t) = n_{i\uparrow}(t)$ for $|U| \leq 0.5$, where $n^b_{i\uparrow}(t)$ is the density of purely ballistic particles (see supplementary material). The definition of the core then corresponds to the diffusive part of the cloud in the model of [9]. The core expansion velocity is given by $\dot{R}(t)$, where $R(t) = \sqrt{< i^2 > - < i >^2}$, $< i >= \sum_{i=1}^{L}([n^C_{i\uparrow}(t) + n^C_{i\downarrow}(t)] * i)/\sum_{i=1}^{L}(n^C_{i\uparrow}(t) + n^C_{i\downarrow}(t))$ and L is the number of lattice sites. The core expansion speed as a function of interaction is plotted in Fig. 9. The behavior of $\dot{R}(t)$ is indeed similar to the core expansion velocity in Fig. 5 of [9], showing also the negative velocities.

Another recent experiment [10] studied collision dynamics of two Fermi gas clouds. Although the experiment is not done in a lattice, the theoretical framework presented here can in the low density limit be used to desribe also physics in [10], c.f. [19].

In conclusion, we studied the expansion of an interacting fermionic gas in a 1D lattice. We showed that the time evolution of this system can be described in terms of a two-fluid model of unpaired particles and doublons whose interplay gives rise to nontrivial dynamics. We suggest that the experimental results of [9] can be interpreted in terms of the analysis performed here. Our results should be widely applicable since expansion is a basic dynamics problem related to the ultracold gas experiments in particular, and to the transport properties of fermions in general.

We thank I. Bloch and U. Schneider for useful discussions. This work was supported by the Academy of Finland (Projects Nos. 213362, 217043, 217045, 210953, 135000, and 141039) and EuroQUAM/FerMix, and conducted as a part of a EURYI scheme grant (see www.esf.org/euryi). The research was partly supported by the National Science Foundation under Grant No. PHY05-51164. This work was supported by ERC (Grant No. 240362-Heattronics). Computing resources were provided by CSC - the Finnish IT Centre for Science.

Note added: After submission of this work, a related numerical study of 1D dynamics has appeared [20].

* Electronic address: paivi.torma@hut.fi

[1] F. H. L. Essler, H. Frahm, F. Göhmann, A. Klümper, and V. E. Korepin, *The One-Dimensional Hubbard Model* (Cambridge University Press, 2005).

[2] K. L. Hur and T. M. Rice, Ann Phys-New York **324**, 1452 (2009).

[3] D. Jaksch and P. Zoller, Ann Phys-New York **315**, 52 (2005).

[4] I. Bloch, Nature Physics **1**, 23 (2005).

[5] M. Greiner, et al., Nature **415**, 39 (2002).

[6] R. Joerdens, et al., Nature **455**, 204 (2008).

[7] U. Schneider, et al., Science **322**, 1520 (2008).

[8] Y. an-Liao, et al., Nature **467**, 567 (2010).

[9] U. Schneider, et al., arXiv: 1005.3545v1, (2010).

[10] A. Sommer, et al., arXiv: 1101.0780v1, (2010).

[11] T. Giamarchi, *Quantum Physics in One Dimension* (Oxford University Press, 2003).

[12] C. Kollath, U. Schollwöck, and W. Zwerger, Phys. Rev. Lett. **95**, 176401 (2005); F. Heidrich-Meisner, et al., Phys. Rev. A **78**, 013620 (2008); F. Massel, M. J. Leskinen, and P. Törmä, Phys. Rev. Lett. **103**, 066404 (2009); F. Heidrich-Meisner, et al., Phys. Rev. A **80**, 041603 (2009); A. Yamamoto, M. Yamashita, and N. Kawakami, J Phys Soc Jpn **78**, 123002 (2009); M. Tezuka and M. Ueda, New J Phys **12**, 055029 (2010); A. Korolyuk, F. Massel, and P. Törmä, Phys. Rev. Lett. **104**, 236402 (2010); S. Diehl, et al., Phys. Rev. Lett. **105**, 227001 (2010).

[13] G. Vidal, Phys. Rev. Lett. **91**, 147902 (2003); A. Daley, et al., J Stat Mech-Theory E p. P04005 (2004).

[14] E. Zhao and W. V. Liu, J Low Temp Phys **158**, 36 (2010).

[15] G. Orso, Phys. Rev. Lett. **98**, 070402 (2007).

[16] H. Hu, X.-J. Liu, and P. D. Drummond, Phys. Rev. Lett. **98**, 070403 (2007).

[17] X.J. Liu, H. Hu and P.D. Drummond, Phys. Rev. A **76**, 043605 (2007).

[18] X.W. Guan, M.T. Batchelor, C. Lee, and M. Bortz, Phys. Rev. B **76**, 085120 (2007).

[19] J. Kajala, F. Massel, and P. Törmä, arXiv: 1102.0133 (2011).

[20] S. Kessler et al., arXiv: 1102.1605 (2011).